ELSEVIER

Ceramics International 26 (2000) 295–302

CERAMICS INTERNATIONAL

Characterization of grain boundary sliding in a fine-grained alumina–zirconia ceramic composite by atomic force microscopy

L. Clarisse, F. Petit[1], J. Crampon, R. Duclos*

Laboratoire de structure et Propriétés de l'Etat Solide, URA CNRS 234, Bât. C6, Université des Sciences et Technologies de Lille, 59655 Villeneuve d'Ascq Cedex, France

Received 2 January 1999; received in revised form 25 March 1999; accepted 2 May 1999

Abstract

Grain boundary sliding has been investigated on the three kinds of interface during the superplastic deformation of a fine-grained alumina–zirconia ceramic composite by atomic force microscopy. The changes in surface topography on both sides of the same boundaries have been characterized throughout specimen deformation. In the experimented deformation conditions (1325°C, 60 MPa) the three kinds of interface exhibit similar sliding mobilities, within 20%, and in average grain boundary sliding contributes to more than 80% of the total strain. The stress redistribution, associated to the difference in phase ductility, has been estimated. The results are in agreement with the values that can be calculated by an isostrain model or a three phase model. © 2000 Elsevier Science Ltd and Techna S.r.l. All rights reserved.

Keywords: B. Composite; B. Grain boundaries; C. Plasticity; D. Al_2O_3; D. ZrO_2; Atomic force microscopy

1. Introduction

It is now well established that superplasticity of metallic alloys and ceramics mainly results from grain boundary sliding and a connected accommodation process. In ceramics this behaviour has been observed in a wide range of single phase (zirconia [1–4], alumina [5,6], silicon nitride [7], spinel [8]) and two-phase (alumina–zirconia [9–12], zirconia–mullite [13], zirconia–SiC whiskers [14] alumina-graphite [15], Si_3N_4/SiC [16]) materials. It is associated with a grain size typically finer than one micrometer that allows stress concentrations to be released by fast diffusion on small distances. In the case of two-phase materials, plasticity is dependent on both intercrystalline interfaces and interphase boundaries. Under these conditions the description of the composite plasticity, from those of the end-constituents, needs the knowledge of the interphase boundary mobility with respect to those of phase boundaries, a parameter that is difficult to evaluate a priori.

Up to the present little attention has been given in ceramic materials to the influence on superplasticity of various interfaces. The most investigated two-phase ceramics are alumina–zirconia composites for which a consensus about the relative mobility of the three types of boundaries does not really exist. Thus according to Wakai et al. [9] the sliding mobility of intercrystalline Al_2O_3–Al_2O_3 (A–A) interfaces is lower than that of ZrO_2-ZrO_2 (Z–Z) and Al_2O_3–ZrO_2 (A–Z) interfaces in consideration of aggregate formation in the alumina phase; these authors propose that interface mobility could be ordered as: Z–Z ~ A–Z > A–A. By considering the higher ductility of Al_2O_3–ZrO_2 composites when the amount of ZrO_2 increases up to 50%, Okada et al. [18] predicted an easier sliding on Al_2O_3–ZrO_2 interfaces than on Al_2O_3–Al_2O_3 boundaries (A–Z > A–A). With similar arguments, the strength of Al_2O_3/ZrO_2 composites being lower than that of the zirconia constituent, Nieh et al. [19] suggested that the mobility of the Al_2O_3–ZrO_2 interface is much higher than that of the ZrO_2–ZrO_2 interface (A–Z > Z–Z). Finally the relatively good agreement between experimental creep rates of composites and those calculated from creep rates of alumina and zirconia end-constituents by different models [12, 13, 17] that do not take into consideration the

[1] Present address: LAMAC, UVHC, Z.I. du Champ de l'Abbesse, 59600 Maubeuge, France.

* Corresponding author. Tel.: +33-3-2043-4990; fax: +33-3-2043-6591.

E-mail address: richard.duclos@univ-lille1.fr (R. Duclos).

PII: S0272-8842(99)00056-5

influence of interphase boundaries suggested us that the three kinds of boundary should have similar sliding mobilities [12].

Consequently the goal of this paper is to investigate the role played by intercrystalline and interphase boundaries during deformation of a superplastic alumina–zirconia composite [12] by direct measurement of the grain boundary sliding on the different interfaces. Such determinations have been already carried out in metallic alloys [20–23]; they showed that the sliding magnitude was dependent on both the kind of boundary and deformation conditions. In those works, authors determined the relative boundary mobility by measuring after deformation either the average step height perpendicular to the specimen surface, by an interferometric method [20], or the offset of marker lines [21–23] on the three types of boundary. These methods are well adapted for materials with grain sizes larger than a few micrometers; however their transposition to fine-grained ceramics is problematic due to the difficulty of measuring very small offsets in marker line [24] or the resolution limit of optical interferometry [25]. Under these conditions we have chosen to analyse the surface of the specimen and its evolution with strain with an atomic force microscope (AFM) in contact mode. The microscope acts then as a high resolution profilometer that allows the measurement of the relative displacement of two neighbour grains in a direction perpendicular to the specimen surface. That method has already proved its interest in the case of a fine grained alumina [26] and presently the relative mobility of each type of interface, as also the sliding contribution to total strain, has been determined. In addition information about the way how adjacent grains move during deformation has been obtained.

2. Experimental procedure

The Al_2O_3/ZrO_2 composite used in this work contained the same volume fraction of each phase (50%). It was sintered at about 1550°C according to the fabrication process described in detail elsewhere [12], and it corresponds to the AZ50 material. The mean linear intercepts of alumina and zirconia grains are $\bar{L}_A = 0.67$ μm and $\bar{L}_Z = 0.48$ μm, respectively, in agreement with grain sizes measured in [12] from determination of average grain area, and the average linear intercept grain size is $\bar{L} = 0.57$ μm.

Compression specimens (7 × 3 × 3mm) were cut and one of the faces was diamond polished and then grain boundaries were thermally etched. After examination by scanning electron microscopy (SEM), one of the specimen was selected for evaluation of the grain boundary sliding after deformation. The specimen was crept at 1325°C under a stress of 60 MPa in four steps corresponding to compressive strains equal to 4.5, 10, 14 and 18%, respectively. The creep rate was about 1.5×10^{-5} s^{-1}. The specimen surface was observed by AFM (Nanoscope III, Digital Instruments) prior to creep and after each strain increment; nevertheless after deformation only the images corresponding to 10 and 18% strains were extensively analysed.

More than 200 boundaries of each type (Al_2O_3–Al_2O_3, ZrO_2–ZrO_2 and Al_2O_3–ZrO_2) were characterized and the grain boundary sliding component perpendicular to the specimen surface (the component v in Fig. 1.) was determined. To this end the image was first filtered and then profiles of the specimen surface in a direction perpendicular to boundaries were drawn. Two cases occurred:

1. for large grains it was generally possible to ajust a plane with their average surface; determination of the vertical offset v was then carried out according to Fig. 2a;
2. on the other hand when small grains were implied, their surface was often curved; in that case we considered the top of the grain as Fig. 2b shows.

Presently, contrary to our previous work [26], the same areas (10 × 10 μm areas) were examined and compared before and after deformation. This allowed us to examine the same boundaries as deformation proceeded. Consequently in each case, the sliding magnitude at a given strain corresponds to the change in step height (considered in absolute value) that occurred between the unstrained state and this strain (for instance $|v_{10} + v_0|$ in Fig. 2a and $|v_{10} - v_0|$ in Fig. 2b). Examination of the same boundaries at the same place, associated with the relatively small increments between two consecutive observations, offered the advantage to make easier and more reliable the measurement of the sliding amplitude by the possible comparison with the previous state.

3. Results

Analysis of the same zones after each strain increment allowed us to observe the changes in specimen topography

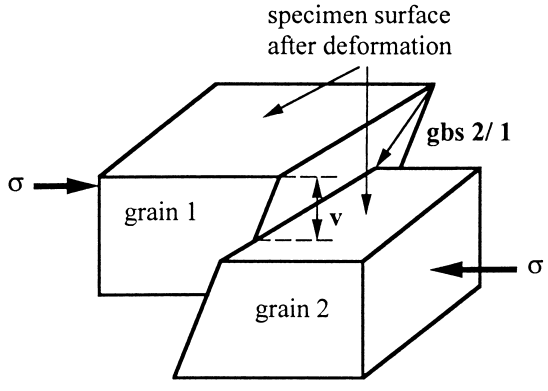

Fig. 1. Definition of the component v of the grain boundary sliding.

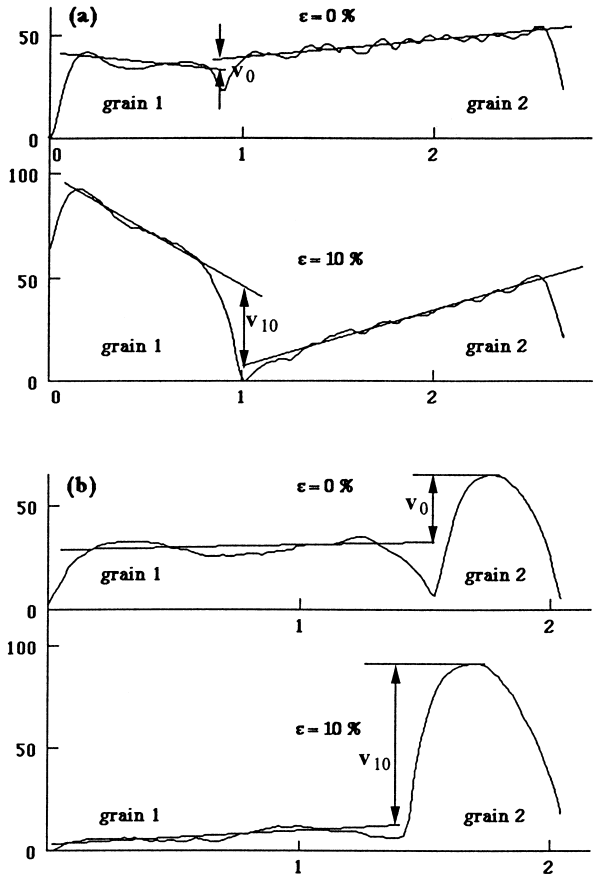

Fig. 2. Two examples showing the procedure used to measure the boundary offset; (a) case of two alumina grains and (b) case of an alumina grain (1) and a zirconia grain (2). The horizontal scales are in μm, the vertical scales in nm.

associated with deformation. These are illustrated in Fig. 3 that shows a same 5 × 5 μm area prior to creep (a) and after strains of 10 (b) and 18% (c), respectively. Grain boundary sliding is very perceptible on the images by the relief evolution and the increase in z range (the coordinate perpendicular to the specimen surface) that are induced. Extensive grain rotations can be also observed in places (see also Fig. 2a). At 10% strain "bubbles" were sometimes observed on the surface of alumina grains. These are small zirconia inclusions that migrated during deformation from the grain inside towards the grain surface. They do not drastically modify the grain surface and did not disturb the v measurement. Due to the contact mode that has been used, AFM images did not allow to distinguish unambiguously the composite phases: alumina and zirconia grains appear with the same contrast, only dependent on the z coordinate. Even if surface of alumina grains is often corrugated, due to bad cleavage, this criterion is not always adequate, specially for small grains, to discriminate between the two phases. Consequently AFM images have been coupled with SEM images to determine the phase distribution. Fig. 4 shows a surface plot of the same zone at 0, 10 and 18% that accounts for the grain movements occurring during deformation (grains move inwards or outwards of the specimen) and the offsets induced at grain boundaries. The disappearance of a grain at the specimen surface as early as 10% can be equally remarked.

From profiles analysis the vertical component v of the sliding was determined. The results are gathered in Fig. 5 for the three types of interface and the two analysed strains. In these diagrams the v values, obtained from measurements performed in six different areas (about 30 to 35 determinations were performed by area), have been arranged by ascending order to facilitate the comparisons. The increase in v with strain is obvious. These curves are nearly insensitive to the kind of interface. The corresponding distribution functions of v are presented in Fig. 6 in the form of histograms for increments of 40 nm. The three interfaces show very similar behaviours. After a strain of 10% the major part of offsets is in the 0–40 nm range while at 18% a strong decrease in the 0–40 nm range corresponds to a marked increase between 80 and 160 nm. In addition offsets up to 300 nm were also recorded (see also Fig. 5), whatever the kind of interface.

The average value of the component v, $< v >$, is presented in Table 1 as a function of interface and strain. The values of this table are reported in Fig. 7 as a plot of $< v >$ versus strain with, for each kind of interface, a linear fit which shows that $< v >$ is about proportional to strain. The slope value for each interface is calculated in the second line of Table 2 that presents in the third line the sliding rate in a direction perpendicular to the specimen surface. Finally in the last line the contribution γ of grain boundary sliding to total strain ε_{total}, $\gamma = \varepsilon_{gbs}/\varepsilon_{total}$, of each type of interface is calculated when this kind of interface is considered separately. The values of ε_{gbs}, the strain due to sliding, have been calculated from the expression proposed by Langdon [27, 28]:

$$\varepsilon_{gbs,i} = 1.4 < v_i > /\bar{L}_i \quad (1)$$

in which i refers to the type of interface. For the interphase boundaries a linear intercept egal to 0.5 $(\bar{L}_A + \bar{L}_Z)$ has been used.

Lastly, concerning the increase in offset with strain it must be noted that the individual behaviour of boundaries is generally different from the average behaviour. As an example Fig. 8 shows values of v after a 10% strain (arranged by ascending order) and those after a 18% strain for 35 ZrO_2–ZrO_2 boundaries in a 10 × 10 μm area. No simple relation exists between the two sets of values. This result is not particular to this type of boundary or the analysed area.

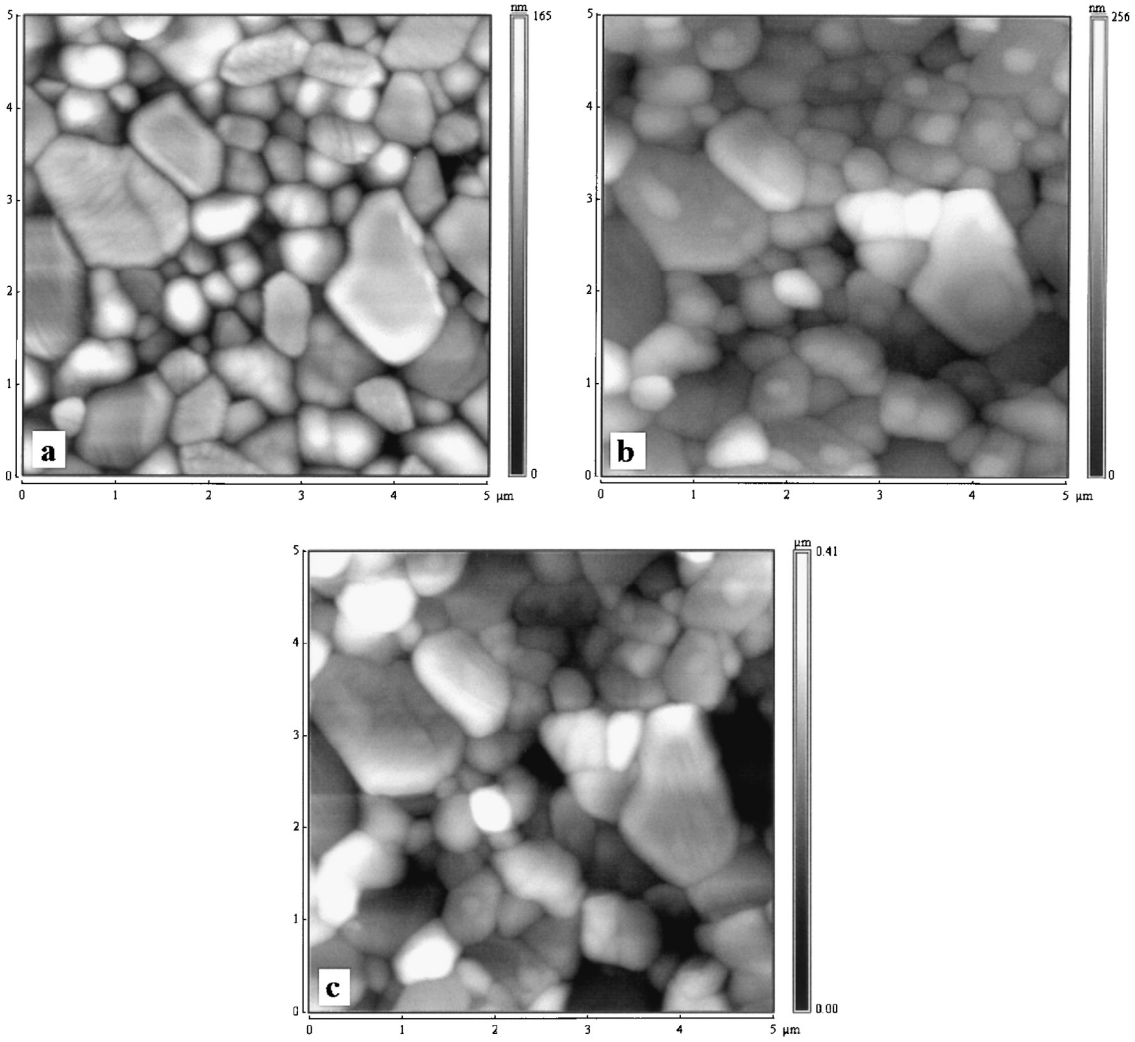

Fig. 3. The same 5 × 5 μm area prior to creep (a) and after strains of 10% (b) and 18% (c), respectively. Note the change in topography and the increase in z range with strain.

4. Discussion

4.1. Limitation of the method

The use and reliability of atomic force microscopy for determination of grain boundary sliding have been already discussed [26]. In the present work the procedure has been improved. The same boundaries were analysed throughout deformation; this method avoids for instance to take into account boundaries whose adjacent grains were not neighbour prior to creep, their offset being not consequently related to a single type of boundary. Besides, the analysis of the same boundaries allowed us to use the same approximation of the grain surface and thus to minimize the scatter related to the fact that, due to fine grain sizes, grain surface is not always flat because of fast surface diffusion, specially in the zirconia phase.

Theoretically this procedure is able to be utilized up to large strains. However elementary processes at the origin of superplasticity can strongly affect the specimen surface and can cause difficulty in the offset estimation. First the neighbour switching event induces grain permutations either in the specimen surface or in a plan perpendicular to the surface. In this last case some grains can disappear (for instance in Fig. 4) or on the contrary new grains can appear. Secondly deformation induces also grain rotation (see Fig. 2a) that are sometimes difficult to take into account. The consequence of these grain movements is a rapid change in surface topology that in practice constrains to limit the analysed strain range to values that do not exceed 20%. Larger strains could be then studied according to the procedure used by Lin et al. [23] that consisted in polishing the specimen surface after a first deformation step and engraving a new set of marker lines.

4.2. Result analysis

From results presented in Tables 1 and 2 two conclusions can be drawn. First the three types of boundary do

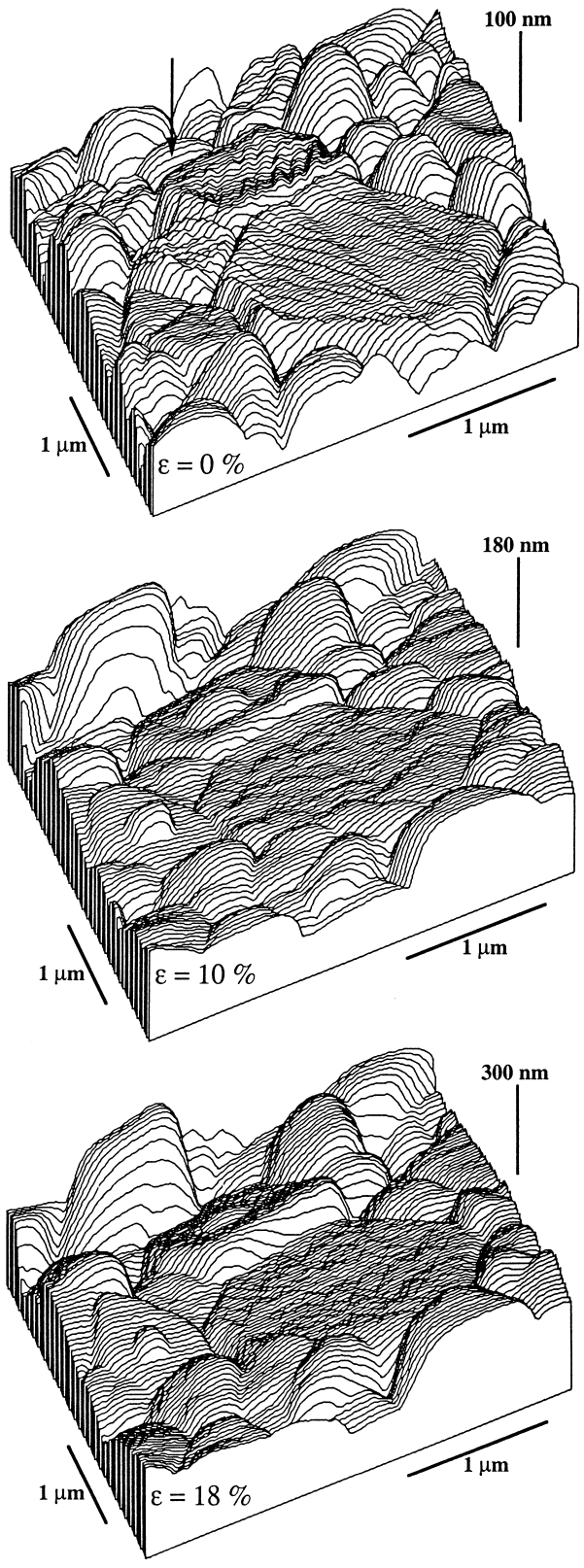

Fig. 4. Surface plots showing offsets associated with deformation. Note the disappearance of a grain after a strain of 10% (arrowed grain at 0%).

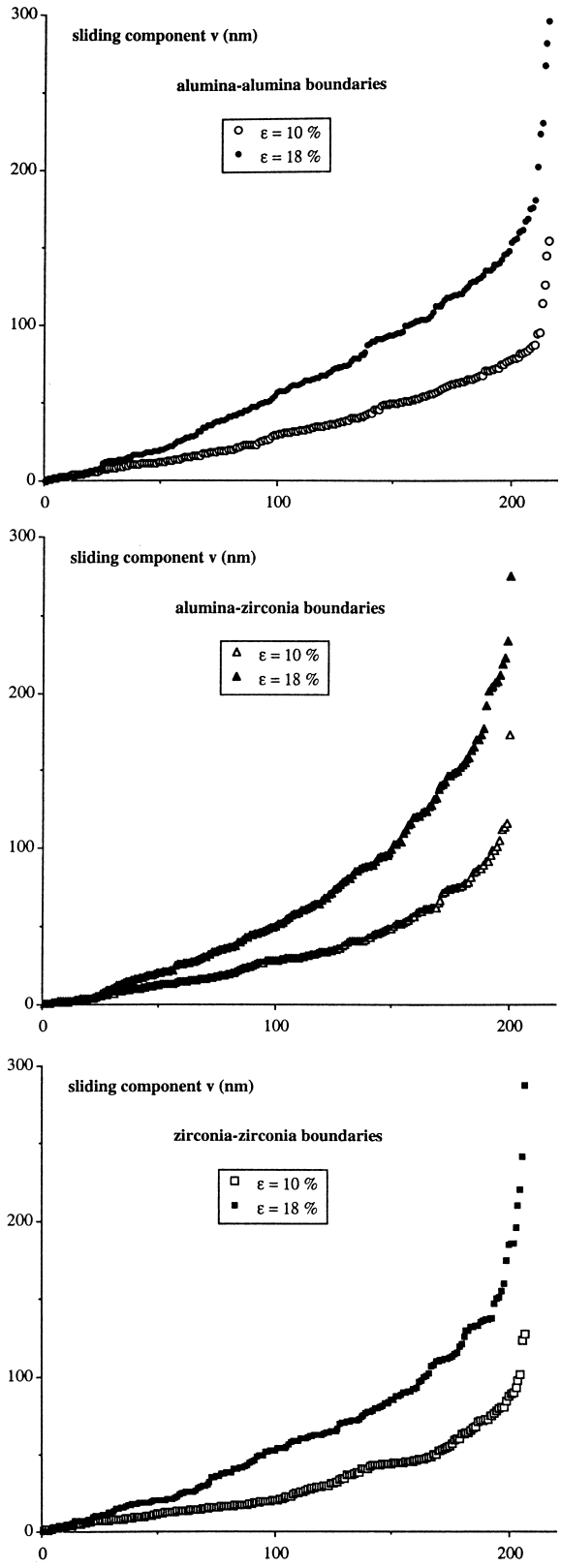

Fig. 5. Plot by ascending order of the sliding component v for more than 200 boundaries of each kind after strains of 10 and 18%.

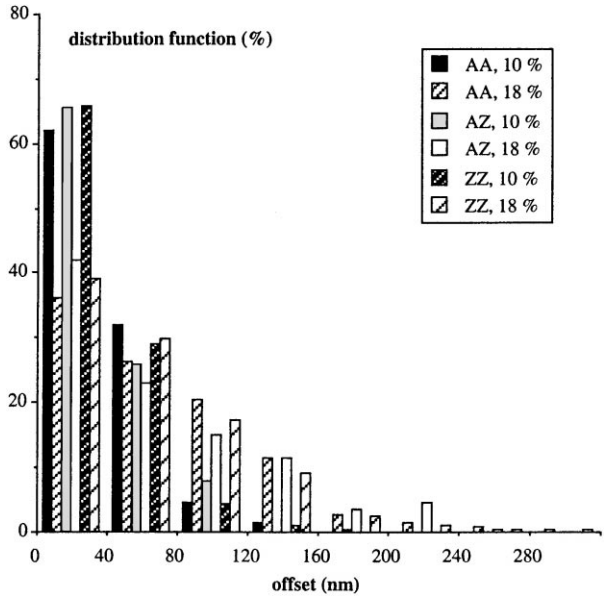

Fig. 6. Distribution function of the component v of sliding versus offset range for the three kinds of boundaries and the two analysed strains.

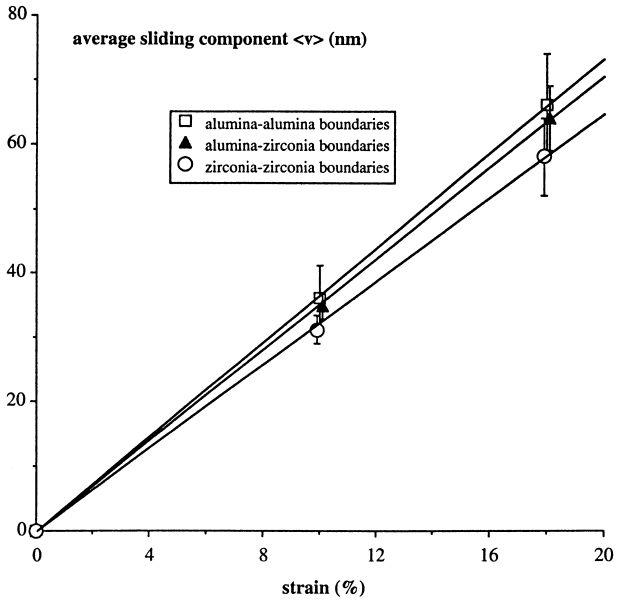

Fig. 7. Plot of average sliding component v versus strain for the three kinds of boundaries with linear curve fits.

Table 1
Average value $< v >$ of the component v as a function of interface kind and strain

Interface	Alumina–alumina		Alumina–zirconia		Zirconia–zirconia		Composite	
Strain (%)	10	18	10	18	10	18	10	18
$< v >$ (nm)	36 ± 5	66 ± 8	35 ± 2	64 ± 5	31 ± 2	58 ± 6	34 ± 3	63 ± 6

Table 2
Influence of the type of interface on three characteristics of the sliding

Interface	Al_2O_3–Al_2O_3	Al_2O_3–ZrO_2	ZrO_2–ZrO_2	Composite
Slope in Fig. 7 (nm/%)	3.6	3.5	3.1	
Sliding rate (nms^{-1})	5.4×10^{-3}	5.2×10^{-3}	4.6×10^{-3}	5.1×10^{-3}
Sliding contribution (%)	75	86	91	84

not exhibit very different sliding capabilities. Sliding rates are within 20% in favour of alumina–alumina interfaces. However due to a finer grain size the sliding contribution is larger in the zirconia phase than in the alumina one. The sliding mobility of interphase boundaries is intermediate between those of intercrystalline boundaries; this observation explains why it is possible to describe the composite behaviour from deformation laws of alumina and zirconia end constituents without taking into account the exact influence of these interphase boundaries. Secondly the contribution of grain boundary sliding to total strain can be estimated to $84 \pm 10\%$. This value emphasizes the important role played by boundaries in the material deformation process; it is consistent with the value expected for a superplastic behaviour. Unless the present contribution is slightly larger than that (about 71%) measured in single phase alumina polycrystals [26], it is not unreasonable; it is likely due to the zirconia phase whose the superplasticity potential is well known and presently to its grain size, finer than the alumina grain size, that renders more propitious the observation of such a behaviour.

In addition to these conclusions which directly issue from offset measurements, the present results can be used to estimate the stress redistribution during deformation. Indeed in the composite the sliding behaviour of a given type of interface is dependent on surrounding grains and necessarily values in Tables 1 and 2 reflect that dependence. Now if we consider an alumina polycrystal with the same linear intercept grain size than the alumina phase in the composite ($\bar{L} = 0.67$ μm) the creep rate for the same deformation conditions (1325°C, 60 MPa) would be 7×10^{-6} s^{-1} see relation (Eq. 4) in [12].

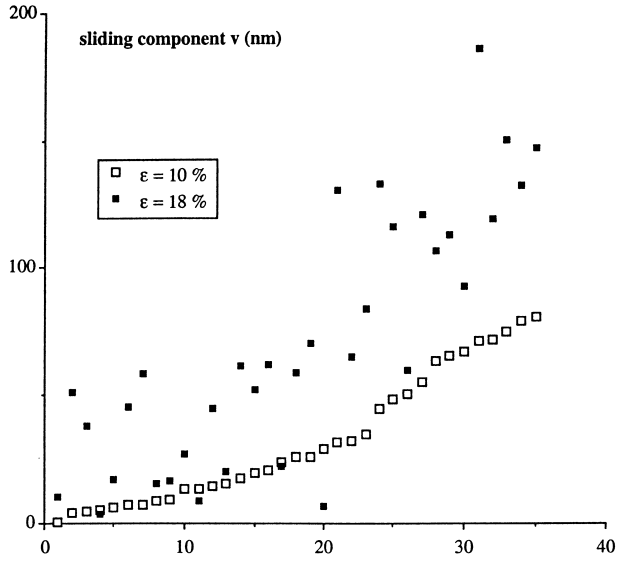

Fig. 8. Comparison of the sliding component v after strains of 10% (classified by ascending order) and 18% for the same 35 zirconia–zirconia boundaries in a 10 × 10 μm area.

Assuming the same contribution of grain boundary sliding than in [26] (71%), the sliding rate would be then 2.5×10^{-3} nm s^{-1}, about half of the sliding rate of alumina–alumina interfaces in the composite (5.4×10^{-3} nm s^{-1}). This higher rate in the composite originates in the stress redistribution that preferentially transfers the applied load on the less ductile phase, presently the alumina phase. A stress of about 100 MPa is thus required to account for the measured sliding rate of alumina–alumina interfaces in the composite. The stress acting on the zirconia phase would be about 20 MPa, such a stress involving in this phase a creep rate of 2×10^{-5} s^{-1} at 1325°C see relation (Eq. 3) in [12]. These stress values are in agreement with those that can be deduced from an isostrain model [17] or the three phase model [29]. They particularly confirm that the composite behaviour can not be described by an isostress model [17].

The present sliding contribution is higher than that reported for metallic alloys in the superplastic region II (60 to 70%) [20–23]. This can come from the small grain sizes of the composite, finer than those reported in metallic materials (at least a factor 2 and generally a factor 10), from the high deformation temperature and also from the fact that intragranular deformation is rendered difficult by the quasi absence of dislocations.

In an alumina–zirconia (80–20 wt%) composite, with linear intercepts equal to 0.85 and 0.40 μm, respectively, the sliding contribution has been estimated by Furushiro et al. [30] to more than 50% of the total strain. However the method used by these authors is not very accurately described; under these conditions the comparison between our results and theirs is difficult.

Concerning the individual boundary behaviour, different from the average behaviour, it shows that grain deformation and specimen deformation are not homothetic, a characteristic that would be observed in Nabarro–Herring or Coble creep when grain boundary sliding is required only to avoid cavity formation. On the contrary this behaviour supports the idea of a non uniform flow and of the driving role of the neighbour switching mechanism in deformation. When locally, conditions become favourable for the achievement of this mechanism, surrounding grains must relax to transmit the strain to specimen volume [31]. The requisite grain movements, and their amplitude, are then not necessarily in phase with the average grain movement owing to the non uniform character of this mechanism inside the specimen. Consequently offsets at 10 and 18% are not necessarily connected.

5. Conclusions

Grain boundary sliding has been analysed in an alumina–zirconia (50–50 vol%) composite on the three kinds of boundary by atomic force microscopy. The microscope has been used in contact mode as a high resolution profilometer that allowed us to observe changes in surface topography throughout specimen deformation. Comparatively to a previous work [26] the method has been improved by characterizing the same boundaries before deformation and after different strains up to 18%.

For the experimented deformation conditions the three types of interface exhibit similar sliding mobility, within 20%. The average contribution of grain boundary sliding to total strain is about 84%, a value that emphasizes the role played by boundaries during deformation. By comparing the sliding rate of alumina–alumina interfaces in this work with the rate obtained in a previous one [26] the stress redistribution, associated to the difference in phase ductility, has been estimated. Thus owing to a lower ductility of the alumina phase the applied stress of 60 MPa is mainly supported by that phase (about 100 MPa), while the stress acting on the zirconia phase is only of the order of 20 MPa. These stress values can agree with those calculated from an isostrain model or a three phase model. They show the interest of such measurements for validation of plasticity modelling of multi-phase materials. Finally determination of grain boundary offset as a function of strain showed that flow inside specimen was essentially non uniform, a feature of superplastic deformation when neighbour switching mechanisms are involved.

References

[1] F. Wakai, S. Sakaguchi, Y. Matsuno, Superplasticity of yttria stabilized tetragonal ZrO_2 polycrystals, Adv. Ceram. Mater. 1 (1986) 259–263.

[2] R. Duclos, J. Crampon, High-temperature deformation of a fine-grained zirconia, J. Mater. Sci. Lett. 6 (1987) 905–908.
[3] C. Carry, A. Mocellin, Structural superplasticity in single phase crystalline ceramics, Ceram. Int. 13 (1987) 89–98.
[4] T.G. Nieh, C.M. McNally, J. Wadsworth, Superplastic properties of a fine-grained yttria-stabilized tetragonal polycrystal of zirconia, Scripta Metall. 22 (1988) 1297–1300.
[5] C. Carry, A. Mocellin, Superplastic forming of alumina, Proc. Br. Ceram. Soc. 33 (1983) 101–115.
[6] F. Wakai, T. Iga, T. Nagano, Effect of dispersion of ZrO_2 particles on creep of fine-grained alumina, Nippon Seramikkusu Kyokai 96 (1988) 1206–1209.
[7] I.-W. Chen, S.L. Hwang, Shear thickening creep in superplastic silicon nitride, J. Am. Ceram. Soc. 75 (1992) 1073–1079.
[8] P.C. Panda, R. Raj, P.E.D. Morgan, Superplastic deformation in fine-grained $MgO{\cdot}2Al_2O_3$ spinel, J. Am. Ceram. Soc. 68 (1985) 522–529.
[9] F. Wakai, H. Kato, S. Sakaguchi, N. Murayama, Compressive deformation of Y_2O_3 stabilized ZrO_2/Al_2O_3 composite, Yogyo-Kyokai-Shi 94 (1986) 1017–1020.
[10] B.J. Kellett, F.F. Lange, Hot forging characteristics of fine-grained ZrO_2 and Al_2O_3/ZrO_2 ceramics, J. Am. Ceram. Soc. 69 (1986) C172–C173.
[11] T.G. Nieh, C.M. McNally, J. Wadsworth, Superplastic behavior of a 20% Al_2O_3/YTZ ceramic composite, Scripta Metall. 23 (1989) 457–460.
[12] L. Clarisse, A. Bataille, J. Crampon, R. Duclos, J. Vicens, Superplastic deformation mechanism during creep of alumina-zirconia composites, Acta Mater. 45 (1997) 3843–3853.
[13] C.K. Yoon, I.-W. Chen, Superplastic flow of two-phase ceramics containing rigid inclusions — zirconia/mullite composites, J. Am. Ceram. Soc. 73 (1990) 1555–1565.
[14] M. Nauer, C. Carry, R. Duclos, Processing of SiC Whisker-reinforced zirconia by extrusion at elevated temperature, J. Eur. Ceram. Soc. 11 (1993) 205–210.
[15] A. Bataille, J. Crampon, R. Duclos, Upgrading superplastic deformation performance of fine-grained alumina by graphite particles, Ceram. Int. 25 (1999) 215–222.
[16] F. Wakai, Y. Kodama, S. Sakaguchi, N. Murayama, K. Izaki, K. Niihara, A superplastic covalent crystal composite, Nature 344 (1990) 421–423.
[17] J.D. French, J. Zhao, M.P. Harmer, H.M. Chan, G.A. Miller, Creep of duplex microstructures, J. Am. Ceram. Soc. 77 (1994) 2857–2865.
[18] K. Okada, Y. Yoshizawa, T. Sakuma, High-temperature deformation in Al_2O_3–ZrO_2, in: S. Hori, M. Tokizane, N. Furushiro (Eds.), Superplasticity in Advanced Materials, The Japan Society for Research on Superplasticity, Osaka, 1991, pp. 227–232.
[19] T.G. Nieh, J. Wadsworth, Superplasticity in fine-grained 20% Al_2O_3/YTZ composite, Acta Metall. Mater. 39 (1991) 3037–3045.
[20] T. Chandra, J.J. Jonas, D.M.R. Taplin, Grain boundary sliding and intergranular cavitation during superplastic deformation of α/β brass, J. Mater. Sci. 13 (1978) 2380–2384.
[21] R.B. Vastava, T.G. Langdon, An investigation of intercrystalline and interphase boundary sliding in the superplastic Pb-62% Sn eutectic, Acta Metall. 27 (1979) 251–257.
[22] P.S. Shariat, R.B. Vastava, T.G. Langdon, An evaluation of the roles of intercrystalline and interphase boundary sliding in two-phase superplastic alloys, Acta Metall. 30 (1982) 285–296.
[23] Z.-R. Lin, A.H. Chokshi, T.G. Langdon, An investigation of grain boundary sliding in superplasticity at high elongations, J. Mater. Sci. 23 (1988) 2712–2722.
[24] A.H. Chokshi, An evaluation of the grain-boundary sliding contribution to creep deformation in polycrystalline alumina, J. Mater. Sci. 25 (1990) 3221–3228.
[25] W. Shin, W.-S. Sea, K. Koumoto, Grain-boundary grooves and surface diffusion in polycrystalline alumina measured by atomic force microscope, J. Eur. Ceram. Soc. 18 (1998) 595–600.
[26] L. Clarisse, A. Bataille, Y. Pennec, J. Crampon, R. Duclos, Investigation of grain boundary sliding during superplastic deformation of a fine-grained alumina by atomic force microscopy, Ceram. Int. 25 (1999) 389–394.
[27] T.G. Langdon, The effect of surface configuration on grain boundary sliding, Metall. Trans. 3 (1972) 797–801.
[28] T.G. Langdon, Grain boundary deformation process, in: R.C. Tressler, R.E. Tressler (Eds.), Deformation of Ceramic Materials, Plenum Press, New York, 1975, pp. 101–126.
[29] E. Hervé, R. Dendievel, G. Bonnet, Steady-state power-law creep in ''inclusion matrix'' composite materials, Acta Metall. Mater. 43 (1995) 4027–4034.
[30] N. Furushiro, T. Tanizawa, K. Akashiro, S. Takeshita, Grain boundary sliding during superplastic deformation in ceramic materials, in: S. Hori, M. Tokizane, N. Furushiro (Eds.), Superplasticity in Advanced Materials, The Japan Society for Research on Superplasticity, Osaka, 1991, pp. 245–250.
[31] M.F. Ashby, R.A. Verrall, Diffusion-accommodated flow and superplasticity, Acta Metall. 21 (1973) 149–163.